J Appl Electrochem (2009) 39:2469–2479
DOI 10.1007/s10800-009-9944-9

ORIGINAL PAPER

Electrochemical behaviour of $Fe_xCo_{3-x}O_4$ with ($x = 0$, 1, 2 and 3) oxides thin film electrodes in alkaline medium

E. Laouini · Y. Berghoute · J. Douch · M. H. Mendonça · M. Hamdani · M. I. S. Pereira

Received: 12 November 2008 / Accepted: 5 June 2009 / Published online: 26 June 2009

Abstract Spinel-type $Fe_xCo_{3-x}O_4$ thin films with $x = 0$, 1, 2 and 3 were prepared, on stainless steel supports, using the thermal decomposition method at 400 °C. The X-ray diffraction patterns show the presence of a spinel-type structure with a low crystallinity. The electrochemical behaviour was investigated in 1 M KOH, using open-circuit-potential measurements and cyclic voltammetry. The studies allowed to observe the redox reactions occurring at the $Fe_xCo_{3-x}O_4$ ($x = 1$ and 2) oxide surface, namely Fe_3O_4/$Fe(OH)_2$ or Fe_3O_4/Fe_2O_3, Co_3O_4/CoOOH, $Co(OH)_2$/CoOOH and CoO_2/CoOOH by comparing the experimental data with those obtained for the Co_3O_4 and Fe_3O_4 films as well as with those referred to in the literature. The results show that iron ions play the major role in the solid-state surface redox transitions in the negative potential range, whereas the cobalt ions are the key species in the positive potential range. However, the contribution of each component, although small, has to be considered in both potential regions.

E. Laouini · Y. Berghoute · J. Douch · M. Hamdani (✉)
Laboratoire de Chimie Physique et Pétrologie, Faculté des Sciences, Université Ibn Zohr, B.P. 8106/S Cité Dakhla, Agadir, Maroc
e-mail: m.hamdani@fs.univ-ibnzohr.ac.ma; hamdani.mohamed@gmail.com

M. H. Mendonça · M. I. S. Pereira
Faculdade de Ciências da Universidade de Lisboa Campo Grande Ed, Centro de Ciências Moleculares e Materiais, C 8, 1749-016 Lisbon, Portugal

M. I. S. Pereira
e-mail: misp@fc.ul.pt

Keywords Mixed cobalt and iron oxide electrodes · Thin films · Cyclic voltammetry · Solid-state surface redox transitions

1 Introduction

Mixed oxides are a wide class of materials, which presents good electro-catalytic activity for many electrode reactions. The availability of different valences of the same metallic element, in these types of materials, is used to modulate the electrode properties through the synergic effects arising from the intimate interaction of the components. Mixed oxides, with a spinel structure and containing cobalt, have been extensively studied, due to their promising catalytic activity for oxygen evolution and reduction (OER) as well as organic electro-oxidation and electro-synthesis [1–3]. Moreover, spinel-type oxides containing iron and cobalt have also generated great interest due to the possible applications as anode materials for batteries [4] and high density recording media [5]. Several studies on the catalytic activity for OER of spinel-type oxide thin films containing cobalt and iron have been published, namely on cobalt ferrite $CoFe_2O_4$ where the Fe is partially replaced by Ni and or Mn [6], $Fe_xCo_{3-x}O_4$ ($0 \leq x \leq 2$) [7] and ternary ferrites $CoFe_{2-x}Cr_xO_4$ ($0 \leq x \leq 1$) [8]. These studies show that the solid-state surface redox transitions (SSSRT), which take place on electrode surfaces, play a crucial role in their activity. A study on the SSSRT on $FeCo_2O_4$ pelleted electrodes has recently been published by some authors [9]. The results obtained and the few publications on the electrochemical behaviour of $FeCo_2O_4$ and $CoFe_2O_4$ oxides led us to study these oxides as thin films.

In this context, this article presents the electrochemical behaviour of $FeCo_2O_4$ and $CoFe_2O_4$ thin film coatings, in

1 M KOH by cyclic voltammetry. This technique is a powerful and versatile tool for in situ non-destructive characterization of SSSRT occurring at the electrode/electrolyte interface. Thin films were prepared by thermal decomposition of nitrates on stainless steel substrates and the SSSRT taking place on their surfaces were analysed. For comparison, Co_3O_4 and Fe_3O_4 thin films were also prepared and studied.

2 Experimental details

2.1 Oxide films preparation

The required amount of cobalt and iron nitrates was dissolved in 100 mL of distilled water followed by the addition of one drop of concentrated HNO_3, in order to avoid any precipitation of the metal hydroxides. All reagents were of analytical grade (Aldrich or Fluka) and were used as-received without further purification. Scratched stainless steel plates (Goodfellow) with 1 cm × 2 cm × 0.1 cm dimensions were used as a substrate. Prior to use, the steel plates were thoroughly washed with distilled water, ultrasonically cleaned in distilled water and absolute ethanol for 10 min and then dried in air. The pre-treatment of the steel surface, prior to coating, is important for the adherence of the film. The pre-treated steel plates were placed in a drying oven at 60 °C and small drops of the mixed metal nitrates solution were dripped onto the surface using a syringe. When the steel surface became dry, more small drops of the solution were dripped onto the surface and dried. This procedure was repeated 4 to 5 times to cover the entire substrate surface uniformly. Finally, the coated steel plates were annealed at 400 °C for 2 h in a tube furnace in air. Following this procedure, black coloured adherent thin oxide films with loadings ranging between 2.0 and 2.4 mg cm^{-2} and 0.3–0.4-μm thick were obtained. The films were used as-prepared.

2.2 X-ray diffraction analysis

X-ray powder diffraction (XRD) analysis was performed using a Philips X-ray diffractometer (PW 1730) with Cu-Kα radiation ($\lambda_1 = 1.54056$ Å), working at 30 mA and 40 kV and automatic data acquisition [APD Philips (v 3.6 B) software]. The diffraction patterns were collected in the range of $2\theta = 15$–$80°$, at a scanning rate of 0.02 s^{-1}. A graphite-monochromator was used. The diffraction patterns were recorded for the substrate, the as-prepared and used films.

2.3 Electrochemical measurements

2.3.1 Electrodes

All the electrochemical studies were carried out in a conventional three-electrode single compartment glass cell in 1 M KOH (Merck, PA, USA) at 25 °C. The working electrode was of stainless steel/oxide. The back of the electrode was isolated with an inert non-conductive varnish and only a single face of 2 cm^2 was exposed to the electrolyte. The electrical contact was made by using a crocodile clip on a small strip of the stainless steel oxide free.

The potential of the working electrode was measured against a saturated calomel electrode (SCE) (0.240 V vs. standard hydrogen electrode (SHE)), connected through a KCl agar–agar salt bridge, the tip of which was placed as close as possible to the surface of the working electrode, in order to minimize solution resistance between the test and reference electrodes. The counter electrode was a platinum plate of 8 cm^2. The solution was deaerated with N_2 for 20 min just before taking measurements.

2.3.2 Techniques and instrumentation

In situ surface characterization and monitoring of the electrode was done by recording cyclic voltammograms (CVs), in 1 M KOH, at a sweep rate of 10 mV s^{-1} in the potential range of −1.3 V to 0.5 V vs. SCE. The influence of both positive ($E_{\lambda+}$) and negative ($E_{\lambda-}$) potential limits on the voltammetric response of the tested electrodes was analysed. The electrochemical measurements were performed using a Voltalab PRZ 100 Radiometer-Analytical apparatus connected to an IMT 102 interface, controlled by a personal computer through the VoltaMaster software.

3 Results and discussion

3.1 X-ray diffraction analysis

Figure 1a shows representative X-ray patterns for the stainless steel substrate, Co_3O_4 powder and (b) $FeCo_2O_4$ films before and after the electrochemical studies. For all the prepared films, the XRD analysis revealed the presence of a spinel structure characteristic of the deposit. The extra lines, detected for all the XRD patterns, corresponded to the stainless steel substrate. These results indicated that all the deposited films were very thin. After the electrochemical studies, the presence of the spinel structure was observed for all the analysed samples, which led us to conclude that the stability of the spinel oxides was acceptable.

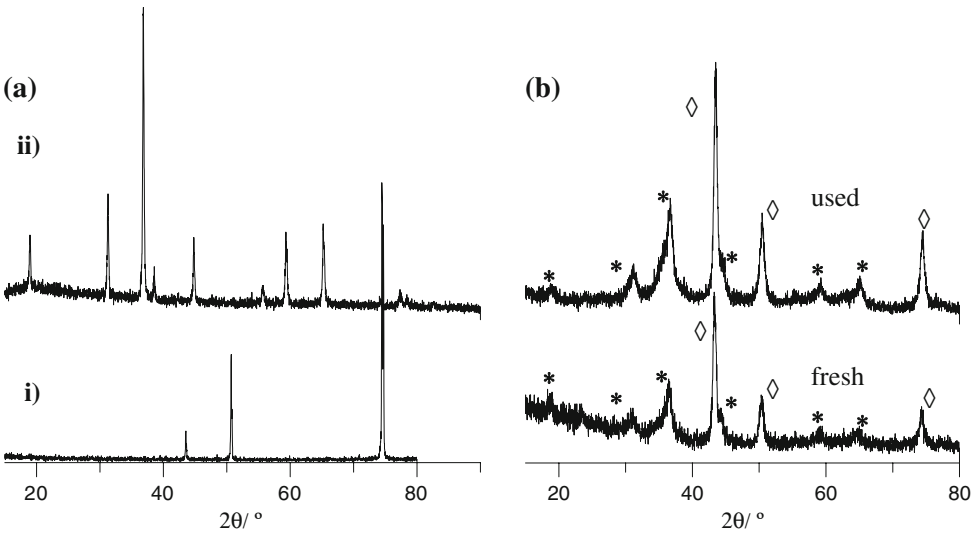

Fig. 1 X-ray diffraction patterns of **a** stainless steel substrate (i), Co_3O_4 powder spinel (ii), **b** $CoFe_2O_4$ films as deposited on stainless steel substrate: fresh **a** and used **b**. Marked peaks ◇ correspond to substrate and ✱ to spinel phase

3.2 Electrochemical studies

3.2.1 Open-circuit potential

Figure 2 shows the dependence of the open-circuit potential (E_{OC}) versus time, in deaerated 1 M KOH solution, for all the prepared electrodes. Two different behaviours are observed. For $x \leq 1$, the E_{OC} increases initially reaching a stable value around −40 mV. For the samples with $x \geq 2$, a different trend is observed. An initial decrease occurs followed by stabilization at −100 mV for $x = 2$ and −150 mV for $x = 3$. The values measured after 240 s indicate that the substitution of Co by Fe in the oxide films tends to lower the electrode E_{OC}. The influence of iron is more pronounced as the amount of iron increases in the oxide. These data are in accordance with the reported value of −0.170 V vs. SCE for $FeCo_2O_4$ pelleted electrodes in 1 M KOH [9]. Silva et al. [10] have shown that the presence of iron oxide in cobalt oxide coatings, on cold-rolled steel films, tends to lower the electrode potential in Na_2SO_4, pH 13. On the other hand, Kishi et al. [7] reported, for $Fe_xCo_{3-x}O_4$, an increase in E_{OC}, with increasing x in Britton–Robinson buffer solutions of pH 6 and 8.

In a recent study, we reported that E_{OC} of Fe–Co_3O_4 (with 0, 5 and 10% of Fe) was 0.000 ± 0.005 V vs. SCE regardless the oxide composition [11]. This result showed

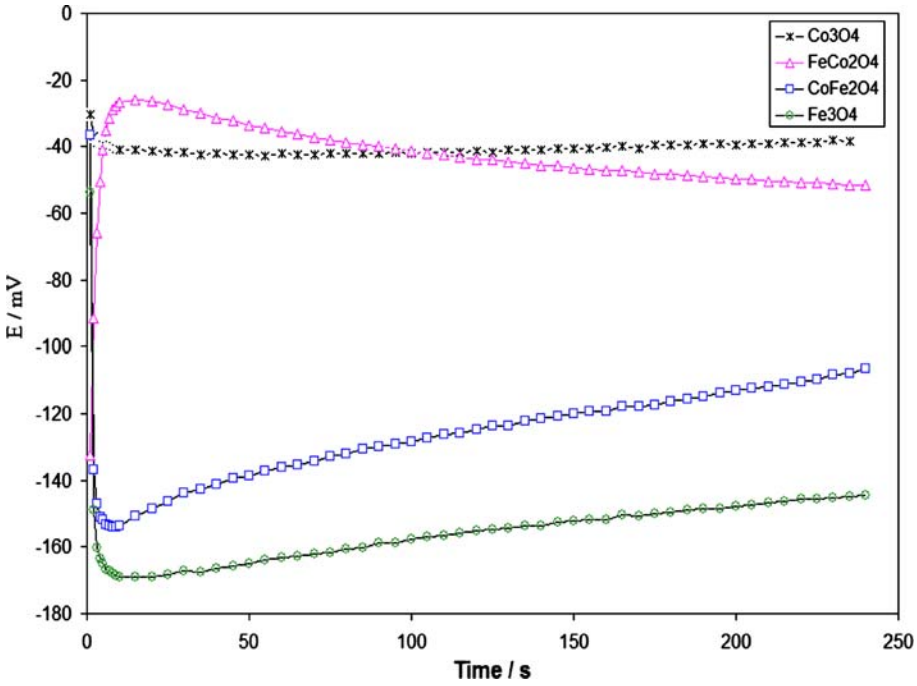

Fig. 2 Open-circuit potential (E_{OC}) versus time, measured for the prepared oxide electrodes, in deaerated 1 M KOH at 25 °C

that the presence of small amounts of iron does not affect the equilibrium redox transitions and consequently the open-circuit potential is mainly governed by the Co^{3+}/Co^{2+} couple as already reported for Co_3O_4 electrodes [12, 13] and that also applies for the samples with $x = 1$. For the enriched iron oxides, $CoFe_2O_4$ and Fe_3O_4 electrodes, the E_{OC} instability values seem to be influenced by the chemical hydrolysis of the oxide surfaces. This process should be slow due to the solution's low penetration rate into the oxide layers [10].

3.2.2 *Voltammetric characterization*

3.2.2.1 General aspects Figure 3 shows the CVs for the Co_3O_4, $FeCo_2O_4$, $CoFe_2O_4$ and Fe_3O_4 thin films in 1 M KOH, starting at 0 V vs. SCE and scanned (a) in the positive and (b) in the negative directions recorded at a scan rate of 10 mV s^{-1}. Considering the positive region for the Co_3O_4 and to a lesser extent for the $FeCo_2O_4$, the CVs exhibit a well-known pair of peaks (A1/C1) prior to the oxygen evolution process, which represents the signature

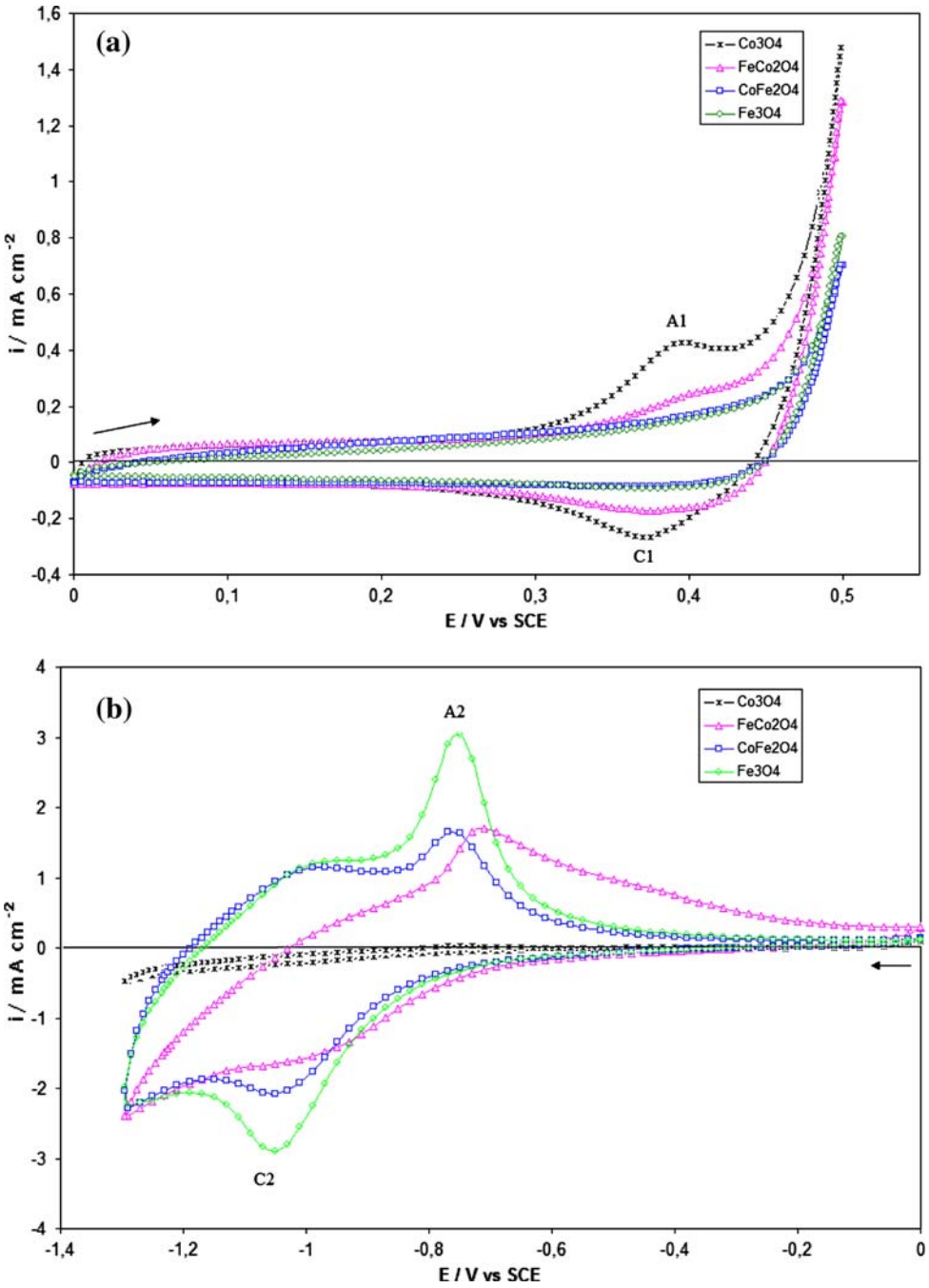

Fig. 3 CVs for Co_3O_4 (*crosses*), $FeCo_2O_4$ (*triangles*), $CoFe_2O_4$ (*squares*) and Fe_3O_4 (*diamonds*) thin film electrodes, in an N_2 deoxygenated 1 M KOH solution at a scan rate of 10 mV s^{-1}, starting at 0 V vs. SCE towards the positive (**a**) and negative (**b**) directions

of the solid state Co^{4+}/Co^{3+} redox couple. The estimated value for the mean peak potential, $E_p = (E_{pa} + E_{pc})/2$ is 0.380 ± 0.005 V vs. SCE for the Co_3O_4. These results are in excellent agreement with those already reported by us [14, 15] for sprayed Co_3O_4/Ti films. The $CoFe_2O_4$ and Fe_3O_4 electrodes do not exhibit any current peak prior to the oxygen evolution but a slight increase in the background current is observed followed by a weak shoulder that overlaps the current due to oxygen evolution. It should be noted that the onset potential for oxygen evolution increased with the cobalt substitution by iron. These results clearly show that cobalt plays the main role in the electrochemical reactions taking place in the positive potential range.

Starting from 0 V vs. SCE in the negative direction (Fig. 3b), no peaks are observed for the Co_3O_4 electrode. The CVs for all the iron-substituted cobalt oxide electrodes exhibit a couple of large current peaks (A2/C2). The peak size and definition increase with the raising of the amount of iron in the oxide film. The CVs for the Fe_3O_4 electrode exhibit both a cathodic and an anodic current peaks, centred at $E_c = -1.100$ V and $E_a = -0.760$ V, respectively.

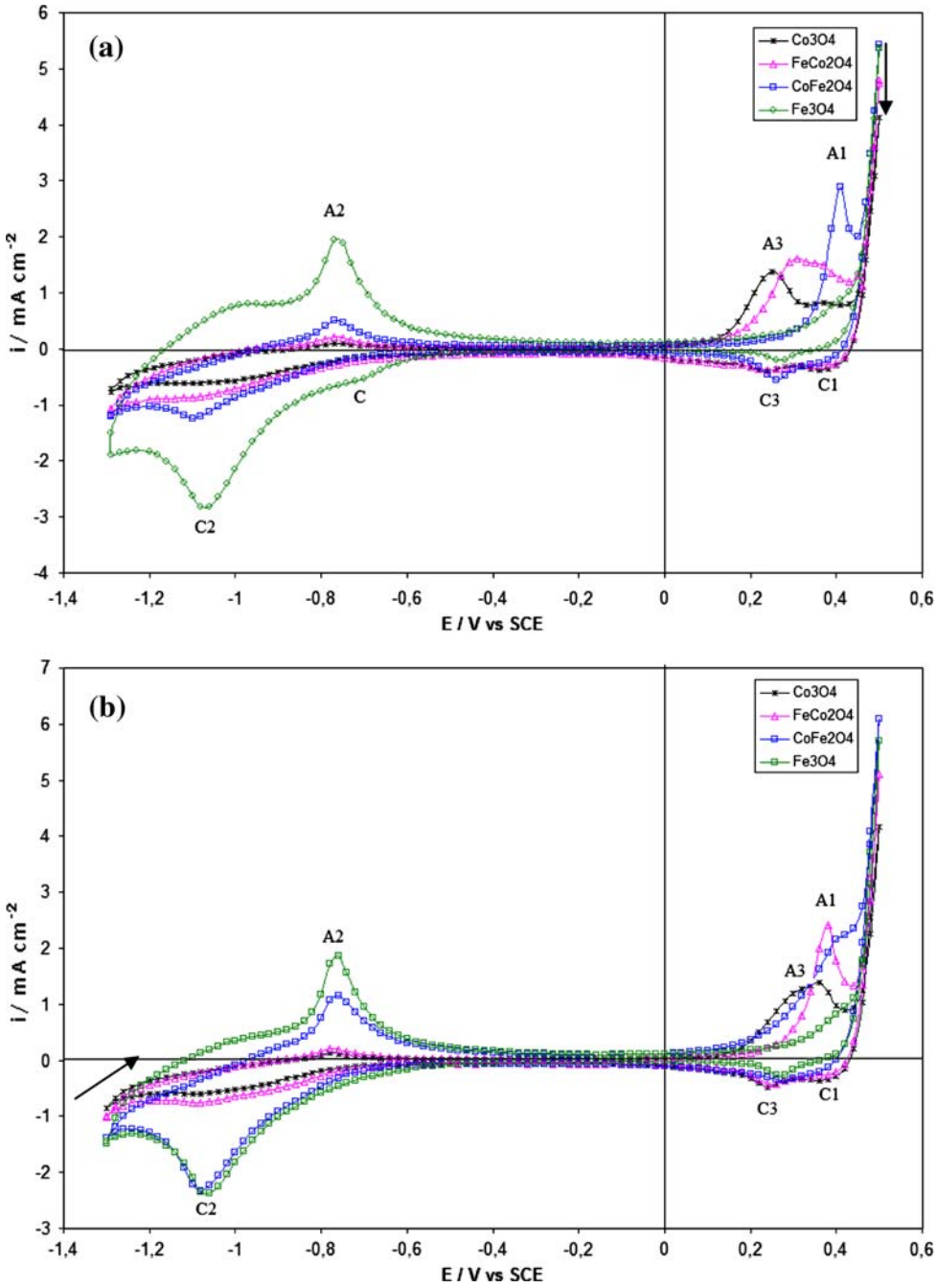

Fig. 4 CVs for Co_3O_4 (*crosses*), $FeCo_2O_4$ (*triangles*), $CoFe_2O_4$ (*squares*) and Fe_3O_4 (*diamonds*) thin film electrodes, in an N_2 deoxygenated 1 M KOH solution at a scan rate of 10 mV s^{-1}, starting at 0.500 V (**a**) and at −1.300 V vs. SCE (**b**)

These peaks are broad, indicating a large heterogeneity on the surface sites due to superposition of the redox processes concerning the metal oxide transitions [16]. As regards to the anodic current profile recorded for the $FeCo_2O_4$, a shoulder follows the anodic peak, where potential is shifted positively in comparison with the corresponding peaks for the $CoFe_2O_4$ and Fe_3O_4 oxide electrodes. In the cathodic scan, the peak is less defined relatively to those obtained for the $CoFe_2O_4$ and Fe_3O_4 oxide electrodes. These results show that iron plays the main role in the electrochemical reactions that take place in the negative potential range.

After these experiments, CVs were recorded for all the prepared oxides, between 0.500 and −1.300 V (Fig. 4), starting at (a) the positive and (b) the negative limits. It is clear that the initial potential does not affect the curve's shape meaningfully. The background currents are very small on all the oxide electrodes, in a large potential window ≈0.700 V, which represents the potential domain where these electrodes are ideally polarizable. The general features in the negative potential range are similar to those recorded previously (Fig. 3b) regardless of the sharpness of the peaks. However, a new pair of shoulders appears for the Co_3O_4 electrode between −0.760 and −1.100 V. For the Fe_3O_4, the formation of a weak shoulder (denoted by C) appears on the cathodic scan below −0.600 V which is attributed to oxygen reduction. On the positive potential range, the voltammetric profiles are more structured than those recorded previously between 0 and 0.500 V (Fig. 3a) and new peaks/shoulders are formed for all the electrodes, being more evident for those containing higher amounts of

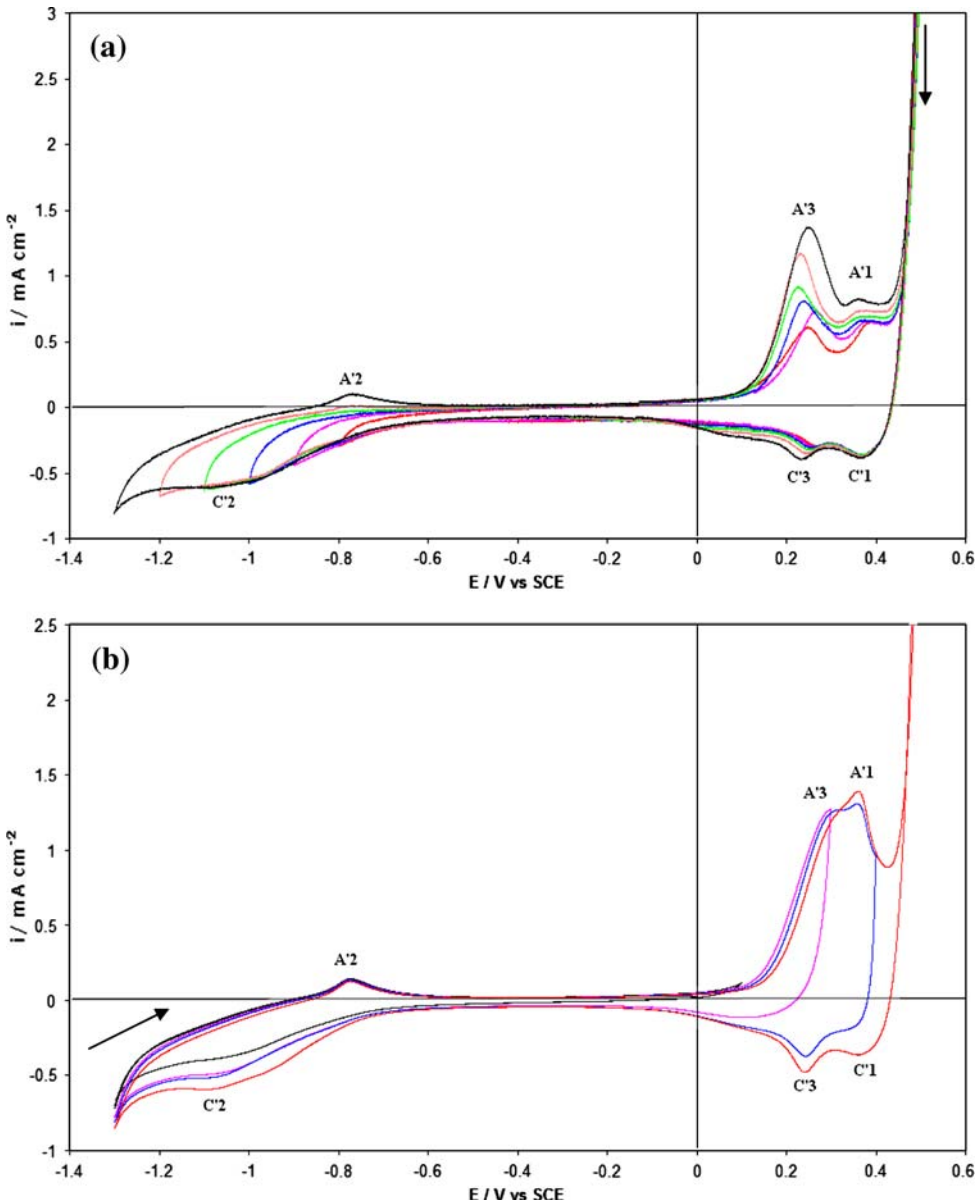

Fig. 5 CVs for Co_3O_4 oxide electrodes obtained in 1 M KOH at a sweep rate of 10 mV s^{-1}, **a** starting at 0.500 V vs. SCE to different negative potential limits and **b** starting at −1.300 V vs. SCE to different positive potential limits

cobalt. Besides, the onset potential for oxygen evolution is the same for all tested electrodes with the appearance of a defined peak before oxygen evolution for the $CoFe_2O_4$ electrode. In contrast for the Fe_3O_4 electrode, no anodic peak is observed. While for the Co_3O_4 and $FeCo_2O_4$ electrodes, one broad peak appears at a lesser positive potential followed by a shoulder. For the negative sweep, similar current profiles were obtained for all the electrodes. Considering Fig. 4b for $FeCo_2O_4$, a more defined anodic peak is recorded while for the $CoFe_2O_4$ a shoulder replaces the peak observed previously before oxygen evolution.

3.2.2.2 Effect of the scan potential limits on the oxides voltammetric response To assign the obtained peaks for the mixed oxides, a study of the influence on both positive ($E_{\lambda+}$) and negative ($E_{\lambda-}$) potential limits on the voltammetric responses of each oxide electrodes was performed (Figs. 5–8).

Figure 5a shows the influence of the potential limits on the voltammetric behaviour of Co_3O_4 oxide electrode when the starting potential is 0.500 V. Two cathodic peaks appear at ca. 0.370 V (C′1) and 0.220 V (C′3) and another one (C′2) starts to develop when $E_{\lambda-}$ reaches the value of approximately −0.700 V. The size of peak C′1 does not depend on the negative potential limit, while C′3 increases with the decrease in the negative potential limit. In the reverse sweep, a small anodic peak A′2 appears at about −0.760 V, only when $E_{\lambda-} < -1.200$ V. In addition, two well-defined peaks A′1 and A′3 are formed prior to the oxygen evolution process. When the sweep starts at the negative potential −1.300 V (Fig. 5b) the same peaks are formed, although the relative size and definition change,

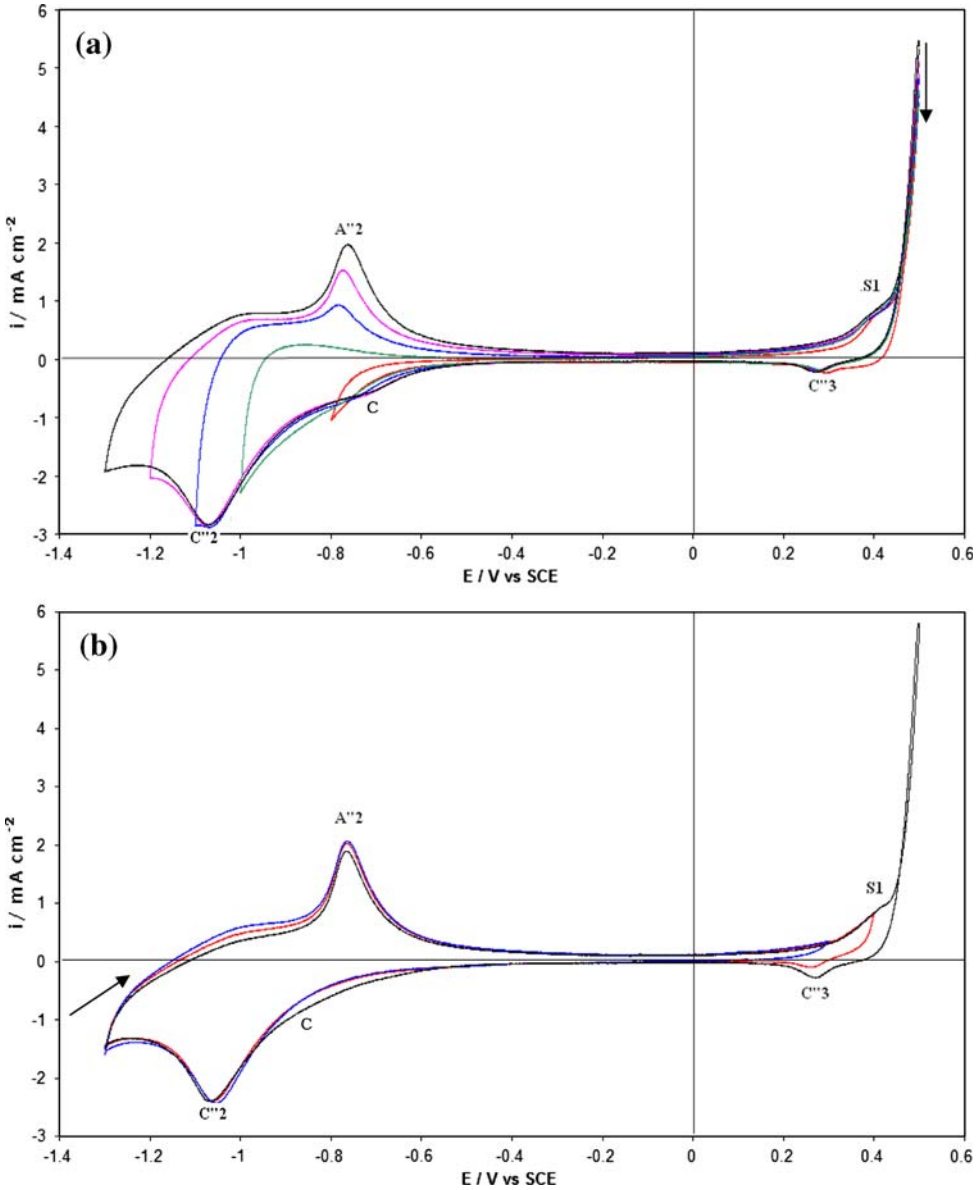

Fig. 6 CVs for Fe_3O_4 oxide electrodes obtained in 1 M KOH at a sweep rate of 10 mV s^{-1}, **a** starting at 0.500 V vs. SCE to different negative potential limits and **b** starting at −1.300 V vs. SCE to different positive potential limits

namely regarding peaks A′3 and A′1. Peak C′3 is associated with both peaks A′3 and A′1, whereas peak C′1 is related to peak A′1. On the other hand, peak A′2 is always present and appears in the negative potential region assigned to the $Fe_3O_4 \cdot 4H_2O/Fe(OH)_2$ couple, although we are dealing with the single cobalt oxide. It could be possible that peak A′2 is due to the reaction of the steel substrate with the electrolyte, since we are dealing with thin porous films. However, the voltammograms recorded for steel and thermally treated steel substrates, which are not shown, do not present any anodic peak in this potential region. This result indicates that peak A′2 is related to redox processes involving cobalt species and or compounds resulting from the interaction between cobalt and the substrate. However, previous results for Co_3O_4 thin films deposited on glass substrates do not present peaks in this potential region [15], which led us to conclude that the peak is due to redox processes involving species resulting from the interaction between the cobalt and the steel substrates.

Regarding peaks A′3/C′3 and A′1/C′1 they should be assigned to Co(III)/Co(II) and Co(IV)/Co(III) redox couples, respectively. Thermodynamic redox potentials corresponding to Co_3O_4/CoOOH or $Co(OH)_2$/CoOOH and CoOOH/CoO_4 are ~0.100 and ~0.420 V vs. SCE that compare well with the experimental peak potentials [13, 17–19]. Peak C′2 could be associated with the reduction of cobalt species in an oxidation state higher than +2, probably a hydrated cobalt oxide, which is difficult to reduce.

The influence of the potential limits on the CVs of Fe_3O_4 is presented in Fig. 6a, b. When the sweep starts on

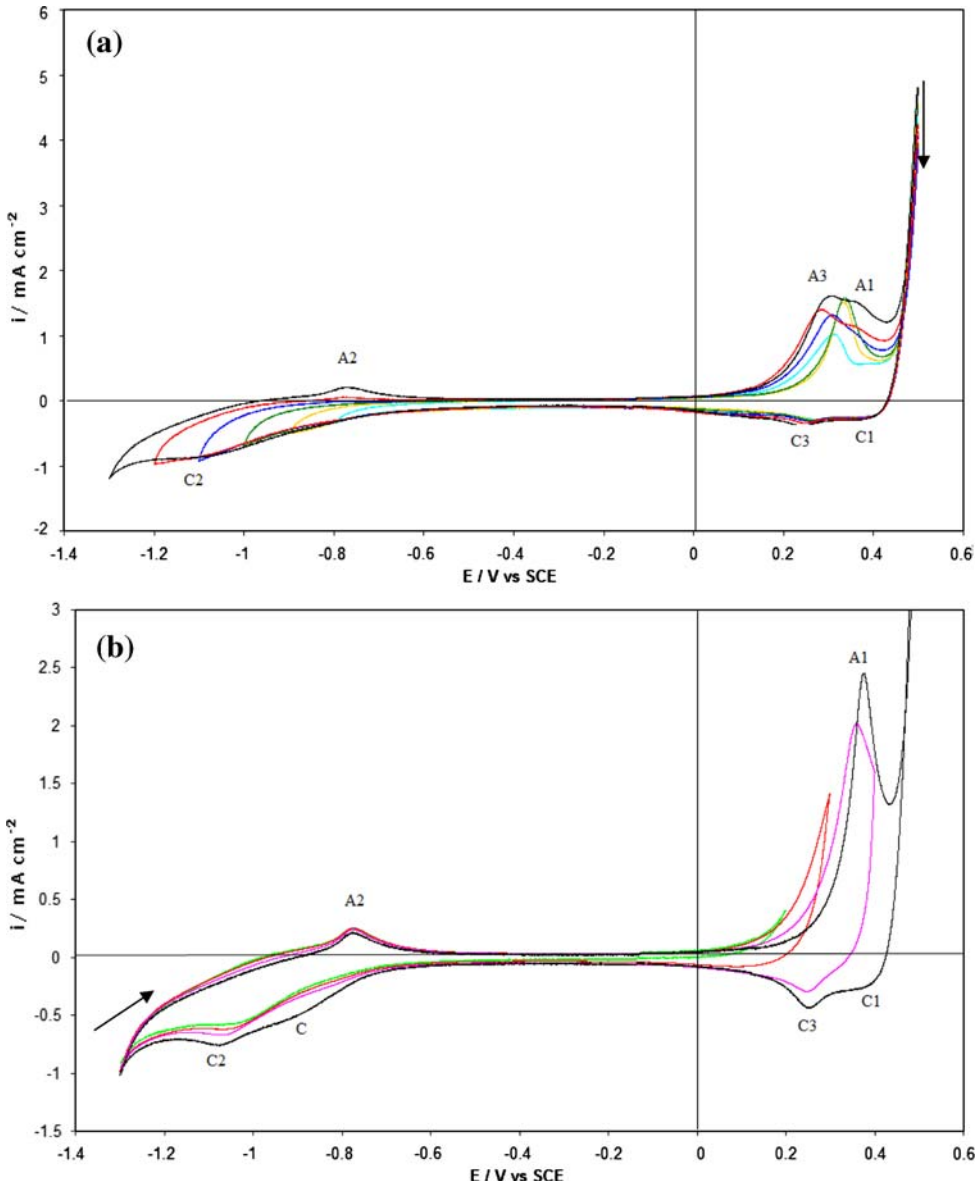

Fig. 7 CVs for $FeCo_2O_4$ oxide electrodes obtained in 1 M KOH at sweep rate of 10 mV s^{-1}, **a** starting at 0.500 V vs. SCE to different negative potential limits and **b** starting at −1.300 V vs. SCE to different positive potential limits

the positive limit, a cathodic peak C″3 is formed at ~0.260 V and another one, C″2, centred at ca. −1.100 V which is associated to the anodic peak A″2 centred at −0.760 V. A shoulder S1 is formed just prior to oxygen evolution. The formation of a weak shoulder (denoted by C) occurs just before C″2. Starting the sweep in the negative limit, the data allowed us to associate peak C″3 to the shoulder S1.

Based on the data so far reported and the information referred to in the literature, peaks A″2/C″2 can be assigned to the redox couple $Fe_3O_4 \cdot 4H_2O/Fe(OH)_2$ for which the calculated equilibrium potential is −0.880 V. This would agree well with our experimental results [20]. Studies for $FeCo_2O_4$ oxides in 1 M KOH, reported by Cartaxo et al. [9], have assigned these peaks to either $Fe_3O_4 \cdot 4H_2O/Fe(OH)_2$ or Fe_3O_4/Fe_2O_3 redox couple. Our results are in good agreement with those reported by Vago and Calvo [21] for Fe_3O_4—PVC composite in 1 M NaOH, and by Allen et al. [22] for magnetite + carbon electrode and assigned to the SSSRT of active species involving the couple of Fe(III)/Fe(II).

The pair S1/C″3 has been attributed to the redox couple FeO_4^{2-}/Fe_3O_4, in accordance with Beck et al. [23]. Other values, for the redox potential of the Fe(VI)/Fe(III), are referred to in the literature namely those of Zhang et al. located between 0.253 and 0.383 V vs. SCE [24–26].

The experiments performed with the single oxides indicate that the redox processes involving either Co or Fe species give rise to anodic (A′2 and A″2) and cathodic (C′3 and C″3) peaks in the same potential regions.

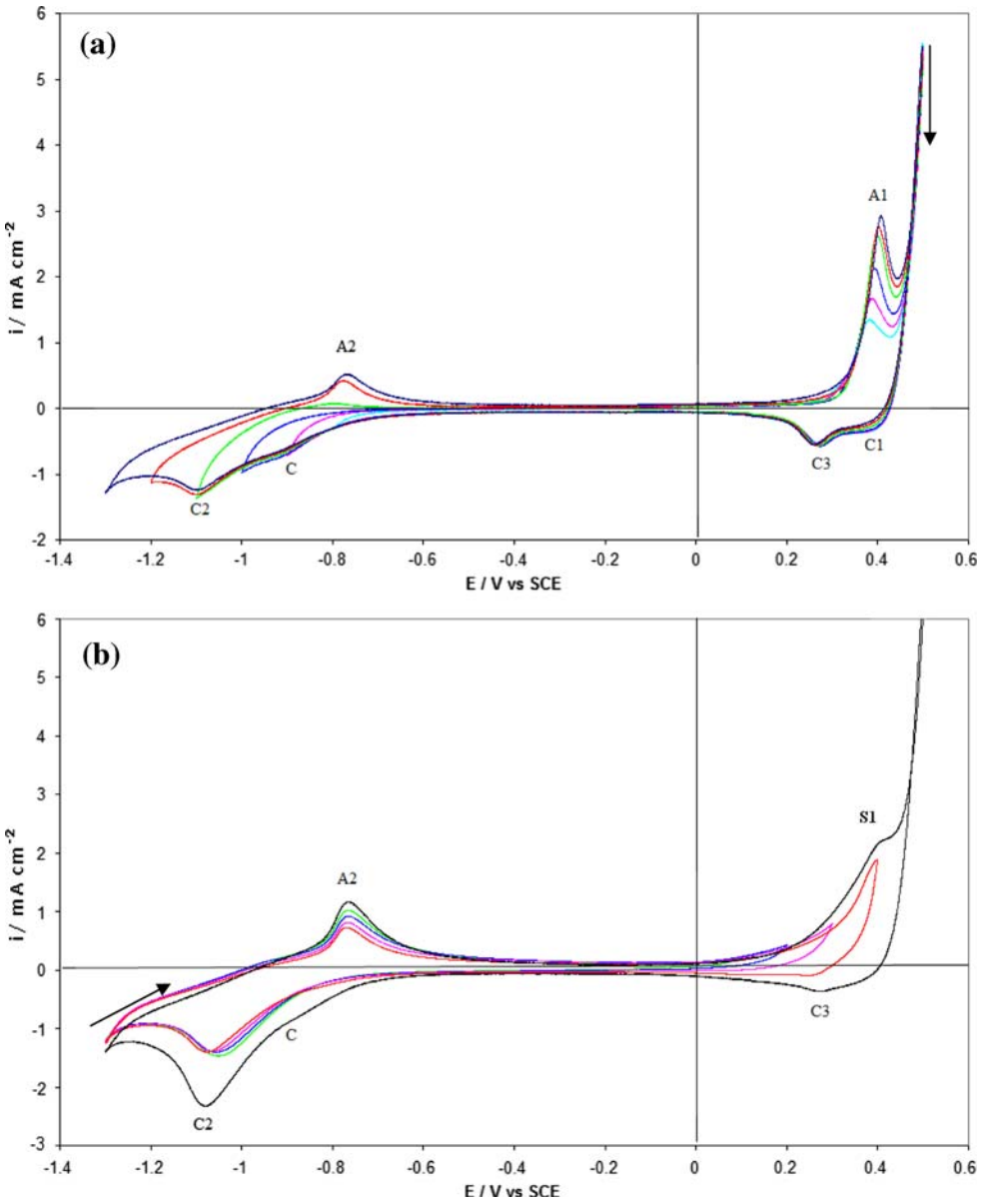

Fig. 8 CVs for $CoFe_2O_4$ oxide electrodes obtained in 1 M KOH at sweep rate of 10 mV s^{-1}, **a** starting at 0.500 V vs. SCE to different negative potential limits and **b** starting at −1.300 V vs. SCE to different positive potential limits

Figure 7a shows the influence of the potential limits for the $FeCo_2O_4$ oxide electrode when the scan starts at the oxygen evolution potential. The voltammetric pattern is similar to the one recorded for the cobalt oxide. The main difference concerns the convolution of peaks A3 and A1. When the sweep starts at the negative potential limit (Fig. 7b), in the positive potential range, only one anodic peak appears (A1), although the two cathodic peaks (C1 and C3) remain without any change.

The results for the $CoFe_2O_4$ electrodes are presented in Fig. 8a, b. The voltammetric patterns are quite different from those recorded for the $FeCo_2O_4$ electrode and resemble those for single iron oxide namely when the sweep starts at the negative potential limit. When the starting potential is 0.500 V the cathodic peaks C1, C3, C and C2 are present. Associated with the appearance of peak C2, the anodic peak A2 is formed presenting the same characteristics as peak A″2 (Fig. 6a). On the other hand, the voltammogram in the positive potential range presents a well-defined peak A1, which increases when the potential limits get more negative and which is characteristic of the cobalt species (Fig. 8a). When the scan starts at the negative potential limit, the most remarkable features are the changes in the size of peak A2 with the positive limit and the disappearance of peak C1. Noting the increase in the size of the shoulder S1 when compared with the one observed for the iron single oxide would indicate the contribution of Co species.

4 Conclusions

It is obvious that for the Fe–Co spinel oxides the electrochemical spectrum is dependent on the composition, namely on the relative amounts of Co and Fe ions. For the oxide with higher amounts of Co ions, the voltammetric patterns approach the ones recorded for the Co_3O_4. Inversely, when the amount of Fe ions is higher the electrochemical behaviour comes close to the Fe_3O_4. It is interesting to note that the peak area is proportional to the iron content in the oxide electrodes in the negative range potential and to the cobalt content in the positive range.

In all cases, iron ions play the main role in the SSSRT taking place in the negative potential range, namely those involving the $Fe_3O_4 \cdot 4H_2O/Fe(OH)_2$ redox couple. Nevertheless, a contribution from Co species, formed at $E < -1.100$ V, cannot be disregarded in this potential region, although the voltammetric pattern is not disturbed by the presence of the cobalt ions. As regards to the positive potential region, where the cobalt species have the key task, the shape and position of the peaks change with the relative amount of iron in the oxide electrode, namely the anodic ones. Indeed a displacement of the peaks, concerning the Co(II) and Co(III) oxidations towards more positive potential is induced by the increase in the amount of Fe ions. However, no meaningful changes are observed for the cathodic peaks. Taking into account the present results, peak A3 was attributed to the oxidation of Co(II) to Co(III) and peak A1 to the oxidation of Co(III) to Co(IV) together with the formation of Fe(VI). Regarding the cathodic peaks, C1 was assigned to the reduction of Co(IV) to Co(III) and C2 to both reduction of Co(III) to Co(II) and Fe(VI) to Fe(III).

Acknowledgement The authors gratefully acknowledge the support of this study by CNRST (Maroc) and GRICES (Portugal) under Research Convention project.

References

1. Trasatti S, Lodi G (1980) In: Trasatti S (ed) Electrodes of conductive metalic oxides, Part B. Elsevier, Amsterdam, p 521 and references therein
2. Tarasevich MR, Efremov BN (1980) In: Trasatti S (ed) Electrodes of conductive metalic oxides, Part B. Elsevier, Amsterdam, p 221 and references therein
3. Trasatti S (1994) In: Lipkowski J, Ross PN (ed) Electrochemistry of novel materials. VCH publishers Inc., New York, p 207 and references therein
4. Alcantara R, Jaraba M, Lavela P, Tirado JL (2002) Electrochemical society meeting, Salt Lake City, p 131
5. Mohan H, Saikh IA, Kulkaarni RG (1992) Solid Sate Commun 82:907
6. Godinho MI, Catarino MA, da Silva Pereira MI, Mendonça MH, Costa FM (2002) Electrochim Acta 47:4307
7. Kishi T, Takahashi S, Nagai T (1986) Surf Coat Technol 27:351
8. Singh RN, Singh NK, Singh JP (2002) Electrochim Acta 47:3873
9. Cartaxo MAM, Ferreira TAS, Nunes MR, Mendonça MH, da Silva Pereira MI, Costa FM (2007) Solid State Sci 9:744
10. Silva GC, Fugivara CS, Tremiliosi Filho G, Sumodjo PTA, Benedetti AV (2002) Electrochim Acta 47:1875
11. Laouni E, Hamdani M, Pereira MIS, Douch J, Mendonça MH, Berghoute Y, Singh RN (2008) Int J Hydogen Energy 33:4936
12. Spinolo G, Ardizzone S, Trasatti S (1997) Electroanal J Chem 423:49
13. Boggio R, Carugati A, Trasatti S (1987) J Appl Electrochem 17:828
14. Hamdani M, Pereira MIS, Douch J, Ait Addi A, Berghoute Y, Mendonça MH (2004) Electrochim Acta 49:1555
15. Singh RN, Hamdani M, Koenig JF, Chartier P (1990) J Appl Electrochem 20:442
16. Mattos-Costa FI, de Lima-Neto P, Machado SAS, Avaca LA (1998) Electrochim Acta 44:1515
17. Hamdani M, Koenig JF, Chartier P (1988) J Appl Electrochem 18:568
18. Longhi M, Formaro L (1999) J Electroanal Chem 464:149
19. Castro EB, Cervasi CA, Vilch JR (1998) J Appl Electrochem 28:835

20. Cordoba SI, Carbonio RE, Lopez Teijelo M, Macagno VA (1986) Electrochim Acta 31:1321
21. Vago ER, Calvo EJ (1992) J Electroanal Chem 339:41
22. Allen PD, Hampson NA, Bignold GH (1979) J Electroanal Chem 99:299
23. Beck F, Kaus K, Oberst M (1985) Electrochim Acta 30:173
24. de Konick M, Bélanger D (2003) Electrochim Acta 48:1435
25. Venkatadri AS, Wagner WF, Bauer HH (1971) Anal Chem 43:1115
26. Zangh C, Liu Z, Wu F, Lin L, Qi F (2004) Electrochem Commun 6:1104